Photophysics of inter- and intra-molecularly hydrogen-bonded systems: Computational studies on the pyrrole–pyridine complex and 2(2′-pyridyl)pyrrole

ARTICLE *in* CHEMICAL PHYSICS · MAY 2008

Impact Factor: 1.65 · DOI: 10.1016/j.chemphys.2007.11.013

2 AUTHORS:

Michal F Rode
Institute of Physics of the Polish Academy o…
31 PUBLICATIONS **420** CITATIONS
SEE PROFILE

Andrzej L. Sobolewski
Polish Academy of Sciences
179 PUBLICATIONS **6,517** CITATIONS
SEE PROFILE

Available online at www.sciencedirect.com
ScienceDirect
Chemical Physics 347 (2008) 413–421
Chemical Physics
www.elsevier.com/locate/chemphys

Photophysics of inter- and intra-molecularly hydrogen bonded systems: Computational studies on the pyrrole–pyridine complex and 2(2′-pyridyl)pyrrole

Michal F. Rode, Andrzej L. Sobolewski *

Institute of Physics, Polish Academy of Sciences, PL-02668 Warsaw, Poland

Received 16 August 2007; accepted 11 November 2007
Available online 28 November 2007

Abstract

The role of electron and proton transfer processes in the photophysics of hydrogen-bonded molecular systems has been investigated with ab initio electronic-structure calculations. We discuss generic mechanisms of the photophysics of a hydrogen-bonded aromatic pair (pyrrole–pyridine), as well as an intra-molecularly hydrogen-bonded π system composed of the same molecular sub-units (2(2′-pyridyl)pyrrole). The reaction mechanisms are discussed in terms of excited-state minimum-energy paths, conical intersections and the properties of frontier orbitals. A common feature of the photochemistry of these systems is the electron-driven proton transfer (EDPT) mechanism. In the hydrogen-bonded complex, a highly polar charge transfer state of $^1\pi\pi^*$ character drives the proton transfer, which leads to a conical intersection of the S_1 and S_0 surfaces and thus ultrafast internal conversion. In 2(2′-pyridyl)pyrrole, out-of-plane torsion is additionally needed for barrierless access to the S_1–S_0 conical intersection. It is pointed out that the EDPT process plays an essential role in the fluorescence quenching in hydrogen-bonded aromatic complexes, the function of organic photostabilizers, and the photostability of biological molecules.

Keywords: Hydrogen bonds; Photophysics; Charge transfer; Proton transfer; Ab initio

1. Introduction

Hydrogen bonds are abundant in organic chemistry and biochemistry. They govern, for example, molecular recognition in DNA and determine to a large extent the secondary structure of proteins. Hydrogen bond interactions play an important role for the catalytic reactivity of enzymes.

While the structure and functionality of hydrogen bonds in the electronic ground state of organic molecules have extensively been investigated with spectroscopic and computational methods [1], very little is known on the photochemistry of hydrogen bonded molecular systems. A notable exception are aromatic systems with an intramolecular hydrogen bond which exhibit the phenomenon of excited-state intramolecular proton transfer (ESIPT) [2–4]. These systems are of considerable applied interest as photostabilizers and sunscreens for the protection of organic polymers and biological tissues [5,6]. Another widely studied phenomenon involving excited-state dynamics of hydrogen bonds is fluorescence quenching in intermolecularly hydrogen-bonded aromatic chromophores [7–10]. A mechanistic explanation of the highly effective deactivation of fluorescent states in terms of curve-crossing dynamics involving a dark charge-transfer (CT) state has been proposed by Mataga [9]. This model remained speculative, however, since it could not be supported by accurate ab initio electronic-structure calculations at that time.

In this work, we have employed the tools of ab initio computational chemistry to explore and compare the primary mechanisms of the photochemistry of intra- and

* Corresponding author. Tel.: +48 22 8436601; fax: +48 22 8430926.
E-mail address: sobola@ifpan.edu.pl (A.L. Sobolewski).

0301-0104/$ - see front matter © 2007 Published by Elsevier B.V.
doi:10.1016/j.chemphys.2007.11.013

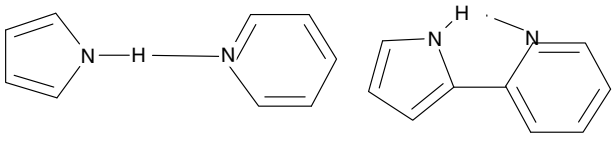

PP 2PP

Scheme 1.

inter-molecularly hydrogen bonded systems. For this purpose we have selected two simple aromatic systems: pyrrole, which models a proton-donating (PD) unit, and pyridine, which represents a proton-accepting (PA) unit. From these molecular bricks, we have constructed the two hydrogen-bonded model systems shown in the Scheme. The pyrrole–pyridine (PP) hydrogen-bonded complex will provide insight into the mechanisms of fluorescence quenching via intermolecular hydrogen bonds. The 2(2′-pyridyl)pyrrole (2PP) molecule, in which two molecular units are connected via a covalent bond, serves as an example of an intramolecularly hydrogen-bonded π-system, for which the mechanisms of the ESIPT process and the function of organic photostabilizers can be investigated (See Scheme 1).

2. Computational methods

The ground-state equilibrium geometries of the rotamers and tautomers of PP and 2PP systems have been determined with the MP2 method. Excitation energies and response properties have been calculated with the CC2 method [11,12]. The equilibrium geometries of the lowest excited singlet states have been determined at the CC2 level, making use of the recently implemented CC2 analytic gradients [13]. Dunning's correlation-consistent split-valence double-zeta basis set with polarization functions on all atoms (cc-pVDZ) [14] was employed in these calculations. The same basis set was used in the calculation of the final vertical excitation energies and oscillator strengths at the optimized geometries (see Supplementary Information (SI)). These calculations were additionally performed with the use of the triple-zeta basis set (cc-pVTZ) in order to check the effect of basis set on the calculated quantities.

The minimum-energy reaction paths along the photophysically relevant reaction coordinates in the ground and in the lowest excited singlet states have been determined with the MP2 and CC2 methods, respectively. For a suitably chosen driving coordinate, all other nuclear degrees of freedom have been optimized for a given value of the driving coordinate. To allow cost-effective explorations of the high-dimensional potential-energy surfaces, the standard split-valence double-zeta basis set with polarization functions on the heavy atoms (def-SV(P)) has been employed in these MP2 and CC2 geometry optimizations. Single-point CC2/cc-pVDZ calculations were performed along the minimum-energy paths on the S_0 and S_1 PE surfaces.

All these calculations were performed with the TURBOMOLE program package [15] making use of the resolution-of-the-identity (RI) approximation for the evaluation of the electron-repulsion integrals [16].

The conical intersections between the S_1 and S_0 energy surfaces have been located at the CASSCF level, using the corresponding module of the GAUSSIAN 03 program package [17]. The active space for the CASSCF calculations consisted of 2 electrons distributed over 2 orbitals (HOMO/LUMO), which have been determined by a restricted Hartree–Fock calculation at an approximate geometry of the conical intersection. At the conical intersection the system is an essentially pure biradical, that is, only two orbitals are singly occupied [18], while all other orbitals have occupation numbers very close to 0 or 2. This justifies the use of a compact active space (2 orbitals /2 electrons) in the CASSCF calculations. The cc-pVDZ basis set was employed in the CASSCF calculations.

3. Results and discussion

3.1. Photoinduced hydrogen transfer in the pyrrole–pyridine complex

The phenomenon of fluorescence quenching through intermolecular hydrogen bonding between aromatic systems is a well-known phenomenon. In numerous studies, Weller, Mataga, Waluk and coworkers have investigated the photophysics of aromatic hydrogen donor-acceptor pairs in various solvents [7–10,19–21]. Mataga has advocated a generic model of fluorescence quenching which emphasizes the role of charge transfer (CT) states which drive proton transfer from the proton donor to the proton acceptor. Curve crossings of the CT state with locally-excited (LE) states facilitate rapid internal conversion [9,19].

We adopt here the pyrrole–pyridine hydrogen-bonded complex for the investigation of excited-state electron and proton transfer processes in hydrogen-bonded aromatic pairs. Two conformers of the pyrrole–pyridine complex were obtained by geometry optimization with C_s symmetry constraint at the MP2/CC-pVDZ level. The two conformers correspond to a parallel and perpendicular arrangement of the aromatic rings, respectively. Both conformers exhibit a fairly strong hydrogen bond (bond lengths are 1.938 and 1.971 Å for the perpendicular and planar forms, respectively). The perpendicular conformer is by about 0.03 eV (0.7 kcal/mol) more stable than the planar conformer. In the following, only the most stable (perpendicular) conformer is considered (Fig. 1a).

The lowest excited singlet states of this conformer result from local excitations within the pyridine ring (Table 1 and Fig. 2). These states can be classified as S_1-LE($\pi\pi^*$) and S_2-LE($n\pi^*$), respectively. The third excited singlet state, S_3-CT($\pi\pi^*$), lies only about 0.1 eV above the S_1 state and has pronounced charge-transfer character, as indicated by its large dipole moment of 18.17 D (Table 1). This state

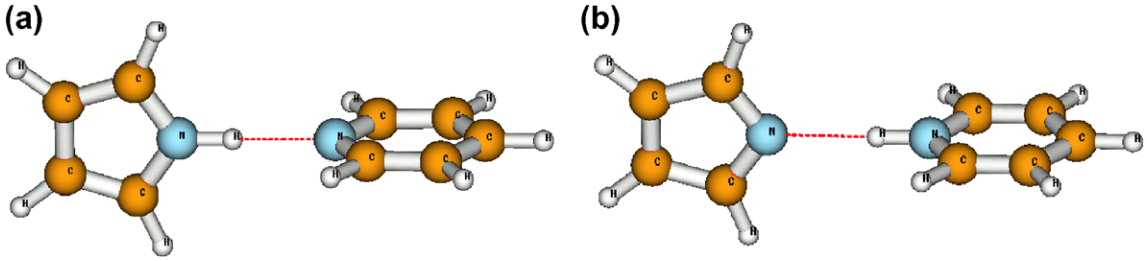

Fig. 1. Ground-state equilibrium geometry (a) and the geometry of the S_0–S_1 conical intersection (b) of the pyrrole–pyridine complex.

Table 1
Vertical excitation energies (ΔE), oscillator strengths (f), dipole moments (μ), and dominant electronic configurations of the pyrrole–pyridine complex calculated with the CC2/cc-pVTZ method at the MP2/cc-pVDZ ground-state equilibrium geometry

State	ΔE/eV	f	μ/D	Electronic structure
S_0	0.0	–	6.02	–
LE($^1\pi\pi^*$)	5.24	0.0300	5.56	$0.84(1a_2 - 9b_2) + 0.52(8b_2 - 3a_2)$
LE($^1n\pi^*$)	5.25	0.0025	1.70	$0.98(20a_1 - 9b_2)$
CT($^1\pi\pi^*$)	5.33	0.0001	18.17	$0.99(2a_2 - 9b_2)$
LE($^1n\pi^*$)	5.60	0.0000	1.59	$0.98(20a_1 - 3a_2)$

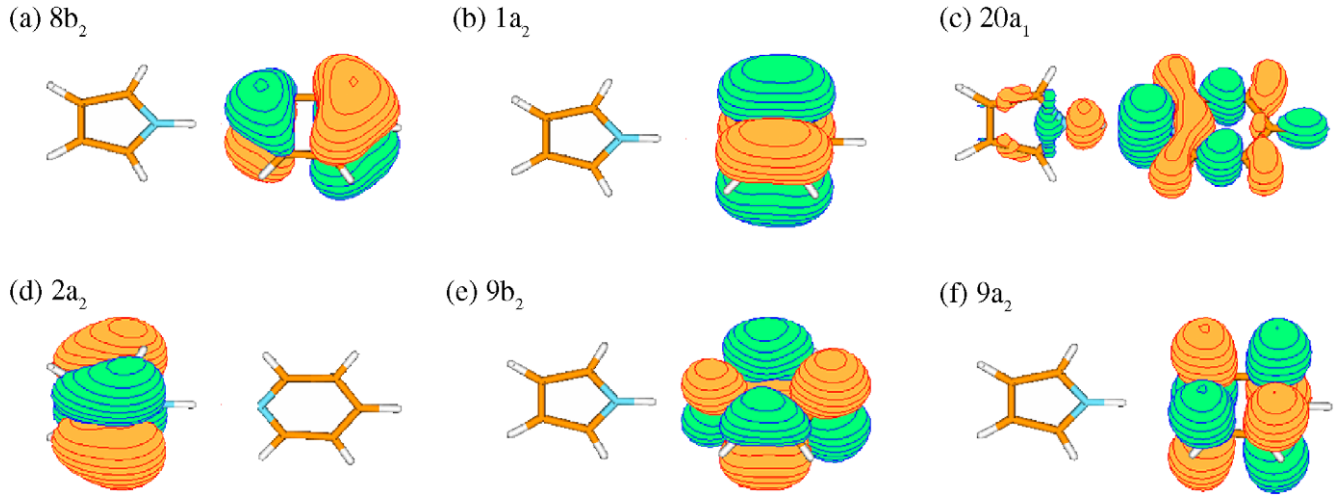

Fig. 2. The three highest occupied π-orbitals (a, b, d), the highest occupied lone pair n orbital (c), and the two lowest unoccupied π^* orbitals (e and f) of the pyrrole–pyridine complex, determined at the equilibrium geometry of the electronic ground state.

involves an electron transfer from the π orbital of pyrrole (Fig. 2d) to the π^* orbital of pyridine (Fig. 2e). Although the CT state is "dark" for direct absorption from the ground state, it can be populated via a non-adiabatic transition from the nearby lying "bright" $S_1(\pi\pi^*)$ state.

The PE profiles for a "rigid" H-transfer from pyrrole to pyridine are shown in Fig. 3a. It is seen that both LE states of pyridine (S_1 and S_2) are crossed by a CT state near their minima. Since both, the S_1(LE) and S_3(CT) states, belong to the same symmetry block, their crossing is actually an avoided crossing. It is noteworthy that the PE energy profile of the CT state is barrierless even for the rigid transfer of the proton (Fig. 3a). Once the CT state is populated, the proton moves from the pyrrole towards the pyridine, following the electron. This reaction is strongly exoenergetic and stabilizes the CT state by about 2 eV. The rigid H-transfer at the equilibrium geometry of the ground state does not result in a crossing of the CT state with the S_0 state, as can be seen in Fig. 3a. An elongation of the distance between the nitrogen atoms of pyrrole and pyridine, from 2.968 Å (the minimum of the S_0 state) to 4 Å, results in a crossing between the states near the minimum of the CT state (Fig. 3b). This *ad hoc* elongation of the intermolecular separation has almost no influence on the location of the LE states, but significantly raises the energy of the CT state near the ground-state minimum and produces a sizable barrier for PT in this state. It is worth to notice, however, that elongation of the intermolecular distance leads to a remarkable stabilization of the energy of a higher excited singlet state, $^1A_2(n\pi^*)$. The PE function of this state develops a minimum approximately half-way between the ground-state structure and the proton-transferred

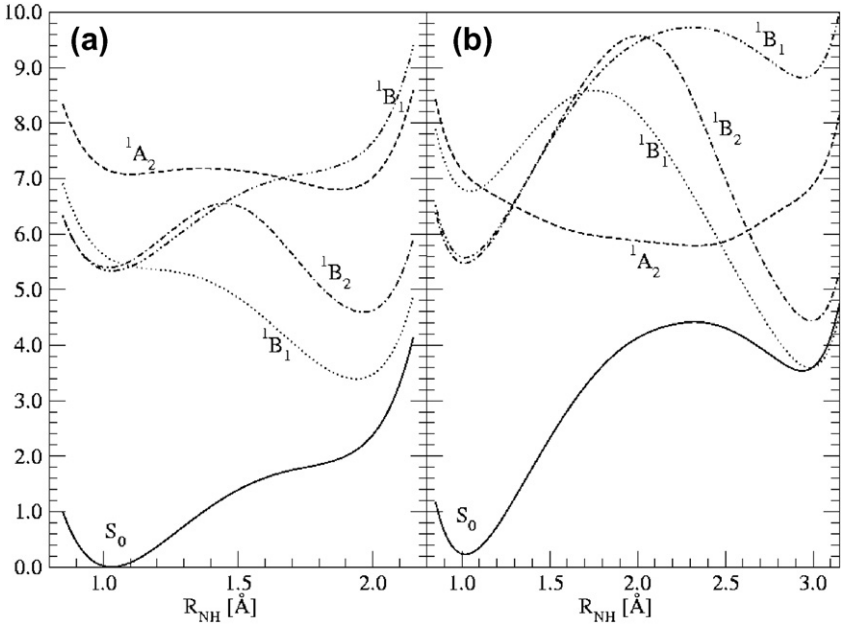

Fig. 3. Potential-energy profiles of the ground and the lowest excited singlet states of the pyrrole–pyridine complex as a function of the proton-transfer ($N_{Pyrrole}H$ stretching) coordinate. (a) Rigid transfer at the ground-state equilibrium geometry; (b) rigid transfer at NN distance stretched to 4 Å.

structure. The PE profile of this state crosses the PE profiles of other excited states much below their barriers (see Fig. 3b). This state thus may be quite important for the photophysical dynamics of this system.

The PE profiles along the minimum-energy path for hydrogen transfer are shown in Fig. 4. The geometry-optimized CT energy crosses both the LE PE function (near its minimum) as well as the PE function of the electronic ground state at larger NH distance. The CC2 method, being a single-reference method, is expected to fail in the vicinity of the intersection of excited states with the electronic ground state. The corresponding regions of the PE profiles are given by dotted lines in Fig. 4, indicating that these data are less reliable. Although the LE–CT crossing is an apparent crossing, since the reaction path was optimized in each state, the CT–$S_0^{(CT)}$ crossing is a true crossing (conical intersection). Since the CT–S_0 conical intersection can be reached directly via a strongly repulsive PE function, we expect a very rapid depopulation of the CT state. The transition from the LE state to the CT state, which may involve a barrier, should be the rate-limiting step in the deactivation of the LE states. Unfortunately, the barrier height resulting from an avoided crossing between the excited states cannot reliably be determined with the aid of a single-reference perturbative method (CC2). To provide upper-limit estimation for the barrier, in Fig. 4 we plot vertical PE profile of the CT state determined along the minimum-energy path of the LE($^1\pi\pi^*$) state. The LE–CT crossing obtained in this way is a real crossing since both PE profiles were calculated at the same geometry. Our results thus point to the conclusion that the barrier for the LE → CT transition is rather small what is in a qualitative agreement with fs/ps time-resolved spectroscopic data of Mataga and coworkers for pyrenol–pyridine and related systems [19]. Fig. 4 fully confirms the qualitative model of fluorescence quenching proposed by Mataga, in particular the role of the CT state which connects the LE($\pi\pi^*$) state with the S_0 state via two conical intersections [9].

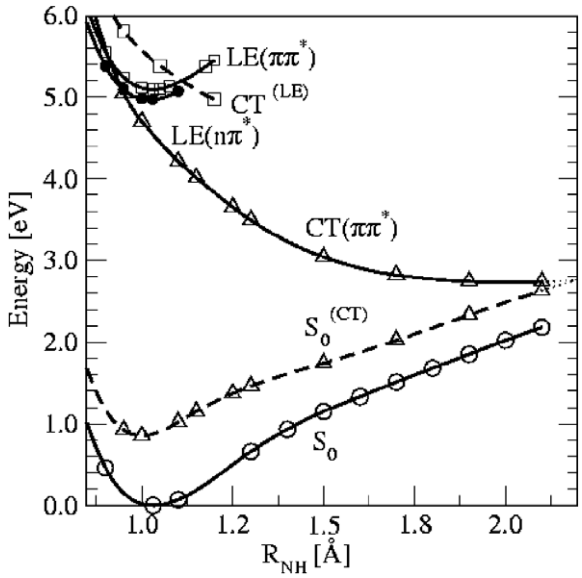

Fig. 4. Potential-energy energy profiles of the S_0 state (circles), and the two lowest locally excited singlet states ($^1n\pi^*$ – dots and $^1\pi\pi^*$ – squares), and the lowest charge-transfer state (triangles) of 2-(2′-pyridyl)pyrrole as a function of the hydrogen-transfer reaction path. Full lines: energy profiles of reaction paths determined in the same electronic state. The dashed line with circles denote the energy of the ground state calculated at the geometry of the CT state (designated as $S_0^{(CT)}$), and the dashed line with squares denote the energy of the CT state determined at geometry of the $^1\pi\pi^*$ state (designated as $CT^{(LE)}$).

Since the CC2 method, being a single-reference method, is not appropriate for the description of the potential-energy surfaces in the immediate vicinity of the conical intersection, we have employed the CASSCF method for the determination of the minimum of the seam of the CT–S_0 intersection, see Section 2. The resulting geometry is shown in Fig. 1b and its Cartesian coordinates are in the SI . The characteristic feature of this geometry is the value of the $N_{pyrrole}\cdots H$ hydrogen-bond length of 2.097 Å. This result confirms the CC2 conjecture that the PE surface of the CT state is crossed by the ground state near its minimum.

The same mechanism has recently been investigated for multiply hydrogen-bonded aromatic pairs, such as the 2-aminopyridine (2AP) dimer [22] and the guanine–cytosine (GC) and adenine–thymine (AT) DNA base pairs [23,24]. Femtosecond time-resolved pump-probe measurements have revealed that the excited-state lifetime is shortened by a factor of 20 in the hydrogen-bonded dimer of 2AP as compared to the monomer [25]. The enhanced excited-state deactivation through hydrogen bonding has been confirmed for the Watson–Crick structure of the GC dimer both in the gas phase as well as in solution [26,27].

3.2. Photoinduced intramolecular hydrogen transfer in 2-(2′-pyridyl)pyrrole

Pyridylpyrroles and pyridylindoles are bifunctional aromatic chromophores possessing both a hydrogen donor as well as a hydrogen acceptor group. Their spectroscopy and photophysics has been studied extensively both in supersonic jets as well as in nonplanar and protic solvents [21,28–30]. Some of the pyridylpyrroles and pyridylindoles studied in these works cannot form intramolecular hydrogen bonds, but are good model systems for the investigation of fluorescence quenching via solvent wires in hydrogen-bonding solvents [29]. 2-(2′-pyridyl)pyrrole (2PP), on the other hand, possesses an intramolecular hydrogen bond in the *syn* configuration, which stabilizes this conformer significantly relative to the *anti* configuration [30]. It has been shown that 2PP shows weak double (blue and red) fluorescence in molecular jets and in nonpolar solvents [30]. The red (tautomeric) fluorescence has been found to decay faster than it is formed. This has been interpreted as evidence that the red fluorescence occurs from the non-relaxed tautomeric form.

The ground-state equilibrium structure of the *syn*-form of 2PP is shown in Fig. 5a (see also SI). It exhibits a weak hydrogen bond (bond length of 2.360 Å) between the azine group of pyrrole and the nitrogen atom of the pyridine ring. The two rings are coplanar at the minimum of the *syn*-form. The *anti* conformer, shown in Fig. 5b, is not planar. The twist angle is 161°. At the CC2/cc-pVDZ level, the *anti* form is located 0.22 eV (4.8 kcal/mol) above the *syn* form (Table 2), and is separated by a barrier of about 0.2 eV (4.6 kcal/mol) from the lower-energy tautomeric *syn* structure.

The hydrogen-transferred *anti* form (with the hydrogen atom attached to the pyridine ring) does represent a very shallow minimum of the S_0 PE surface at the CC2/cc-pVDZ level, with the barrier of about 0.2 eV, but it is expected to be a transient structure on the ground-state PES due to large exoenergeticity (0.8 eV) of the reverse PT reaction.

The *anti* configuration of this tautomer, shown in Fig. 5c, is another local minimum of the S_0 surface. The twist angle of this structure is 180° and the energy is 1.02 eV (25 kcal/mol) above the global S_0 minimum (at

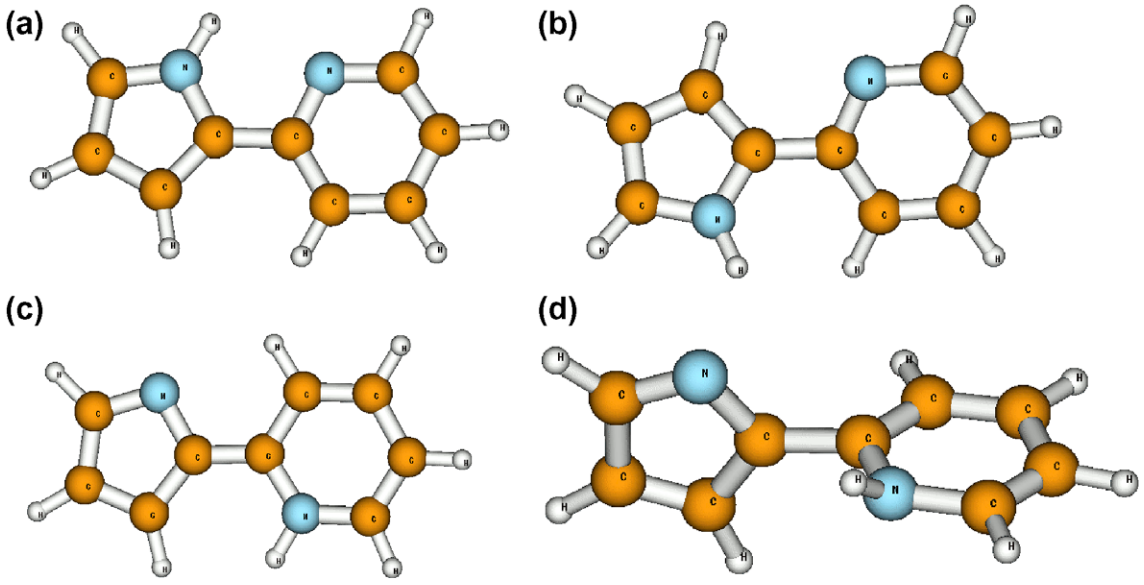

Fig. 5. Ground-state equilibrium geometries of the *syn* (a) and *anti* (b) forms of 2-(2′-pyridyl)pyrrole. The ground-state equilibrium geometry of the hydrogen-transferred structure of the *anti* conformer is shown in (c). The structure (d) shows the geometry of the S_0–S_1 conical intersection.

Table 2
Vertical excitation energies (ΔE), oscillator strengths (f), dipole moments (μ), and dominant electronic configurations of 2(2′-pyridyl)pyrrole calculated with the CC2/cc-pVTZ method at the MP2/cc-pVDZ ground-state equilibrium geometry

State	ΔE/eV	f	μ/D	Electronic structure
Normal syn-form				
S_0	0.0	–	1.24	–
$^1\pi\pi^*$	4.32(4.10)[b]	0.329	4.77	$0.87(\pi_H\pi^*_L) - 0.38(\pi_H\pi^*_{L+1})$
$^1\pi\pi^*$	4.69	0.281	6.00	$0.42(\pi_H\pi^*_L) + 0.82(\pi_H\pi^*_{L+1})$
$^1n\pi^*$	5.13	0.002	2.65	$0.94(n\pi^*_L) - 0.26(n\pi^*_{L+1})$
$^1n\pi^*$	5.39	0.001	2.53	$0.25(n\pi^*_L) + 0.95(n\pi^*_{L+1})$
Normal anti-form				
S_0	(0.22)[a]	–	3.19	–
$^1\pi\pi^*$	4.40(4.14)[b]	0.239	6.39	$0.79(\pi_H\pi^*_L) + 0.49(\pi_H\pi^*_{L+1})$
$^1\pi\pi^*$	4.75	0.360	6.43	$0.55(\pi_H\pi^*_L) - 0.75(\pi_H\pi^*_{L+1})$
$^1n\pi^*$	4.94	0.005	0.98	$0.90(n\pi^*_L) + 0.35(n\pi^*_{L+1})$
$^1n\pi^*$	5.15	0.001	0.72	$0.33(n\pi^*_L) - 0.86(n\pi^*_{L+1})$
Tautomeric anti-form				
S_0	(1.02)[a]	–	5.94	–
$^1\pi\pi^*$	3.02	0.272	3.36	$0.95(\pi_H\pi^*_L) - 0.25(\pi_H\pi^*_{L+1})$
$^1\pi\pi^*/^1n\pi^*$	3.74	0.078	4.11	$0.85(\pi_{H-1}\pi^*_L) - 0.50(\pi_H\pi^*_{L+1})$
$^1\pi\pi^*$	3.83	0.426	3.54	$0.65(\pi_H\pi^*_{L+1}) + 0.65(\pi_{H-1}\pi^*_L)$
$^1n\pi^*$	4.15	0.001	1.58	$0.96(n\pi^*_L) + 0.22(n\pi^*_{L+1})$

[a] Relative to the minimum of the normal *syn*-form.
[b] Adiabatic energy.

the CC2/cc-pVDZ level), but is protected by a sizable barrier of about 1 eV with respect to the reverse PT reaction.

The vertical excitation energies and oscillator strengths of the ground-state isomers of 2PP are given in Table 2 (see also SI). The *syn* form absorbs strongly ($f = 0.33$) in the UV ($\Delta E = 4.32$ eV). The vertical excitation energy of the $S_1(\pi\pi^*)$ state of the *anti* form is 4.40 eV, only slightly shifted to the blue of the *syn* form. The hydrogen-transferred (tautomeric) *anti* form is a photochromic species, since it has a strongly red-shifted absorption spectrum ($\Delta E = 3.02$ eV, $f = 0.27$).

Optimization of the geometry of the $S_1(\pi\pi^*)$ state with C_s symmetry constraint, starting from the ground-state equilibrium geometry of the *syn* conformer, results in a stable structure of a "normal" tautomer which shows a small (about 0.2 eV) barrier for transfer of a hydrogen atom to the pyridine ring. This hydrogen-transferred (tautomeric) structure represents, however, a saddle point on the S_1 PE surface. This structure is unstable with respect to torsion around the central CC bond. The unconstrained optimization of the S_1 energy leads to a minimum-energy structure with a pyrrole–pyridine twist angle of about 90° and a slightly pyramidal N atom of the pyridine ring (the sum of the bond angles is 350°). The energy of this S_1 minimum lies 3.3 eV above the global minimum of the S_0 surface. At this S_1 minimum-energy geometry, the ground-state is only 0.5 eV below the S_1 state (CC2/cc-pVDZ value).

The calculated adiabatic energy of the S_1 state in the normal *syn* tautomer (4.10 eV, Table 2) can only roughly be compared to the (unobserved) 0-0 line in the "blue" fluorescence of 2PP in the jet, which has been estimated to lie at about 4.0 eV [30]. The difference of 0.1 eV is well within the expected error of the CC2 method. A similar difference is found for the vertical energy of the blue fluorescence (3.7 eV – experiment, 4.0 eV – theory). The maximum of the red (tautomeric) fluorescence is observed around 2 eV [30]. Our estimate agrees with this value, if the planar stationary point (the saddle point) on the S_1 PE surface is considered as the emitting state of the tautomeric form. This assignment is consistent with the interpretation of the experiment [30] where the red fluorescence has been interpreted as occurring from the non-relaxed tautomeric form.

Fig. 6 provides an overview of the PE functions of 2PP as functions of the hydrogen-transfer coordinate (NH bond length) and the inter-ring twisting coordinate (NCCN dihedral angle) in the S_0 and S_1 states. These minimum-energy-path profiles were obtained by calculating the CC2/cc-pVDZ energy of the S_0 and S_1 states at geometries which were optimized at the MP2/def-SV(P) and CC2/def-SV(P) levels, respectively. In addition, the energy profiles of the ground state calculated at the optimized geometry of the excited state, $S_0^{(S_1)}$, is shown (dashed lines).

Fig. 6a shows the PE functions for torsion of 2PP. The global ground-state minimum (*syn* form, Fig. 5a) is planar. The *anti* form (Fig. 5b) shows up as a shallow minimum near 160°, separated by a low barrier of about 5 kcal/mol. The torsional barrier is more pronounced in the S_1 state.

The energy profiles for the hydrogen-transfer reaction of the *syn* conformer of 2PP are displayed in Fig. 6b. As is typical for ESIPT systems, the hydrogen-transfer process is endoenergetic in the electronic ground state, but exoenergetic in the S_1 state. In both cases, the minimum-energy-path potential function is almost barrierless. We identified, however, two different LE states of the $\pi\pi^*$ character in the vicinity of the minimum of the *syn* form of the normal tautomer. Their PE profiles exhibit an avoided crossing near $R_{NH} = 1.2$ Å (Fig. 6b). The small barrier associated with this crossing may be responsible for appearance of the blue fluorescence of the system [30]. Beyond the barrier, the PT reaction is strongly exoenergetic, but as mentioned above, the hydrogen-transferred S_1 surface is unstable with respect to torsion around the central CC bond.

The torsional PE functions for the hydrogen-transferred tautomer of 2PP are shown in Fig. 6c. The minimum-energy profile of the S_0 state clearly exhibits a minimum near 180°, which corresponds to the structure of Fig. 5c. The minimum-energy path in the S_1 state could be followed from $\theta = 0°$ (planar system) through the minimum of the S_1 state ($\theta = 90°$) up to $\theta = 180°$. Although the CC2 method, being a single-reference method, is stretched to the limit by these calculations, particularly near the perpendicular configuration of the two rings, the results of Fig. 6c provide strong evidence for the existence of a conical intersection between the S_1 and S_0 surface at a dihedral angle near 90°.

The conjecture resulting from the CC2 calculations is fully confirmed by the optimization of the conical intersec-

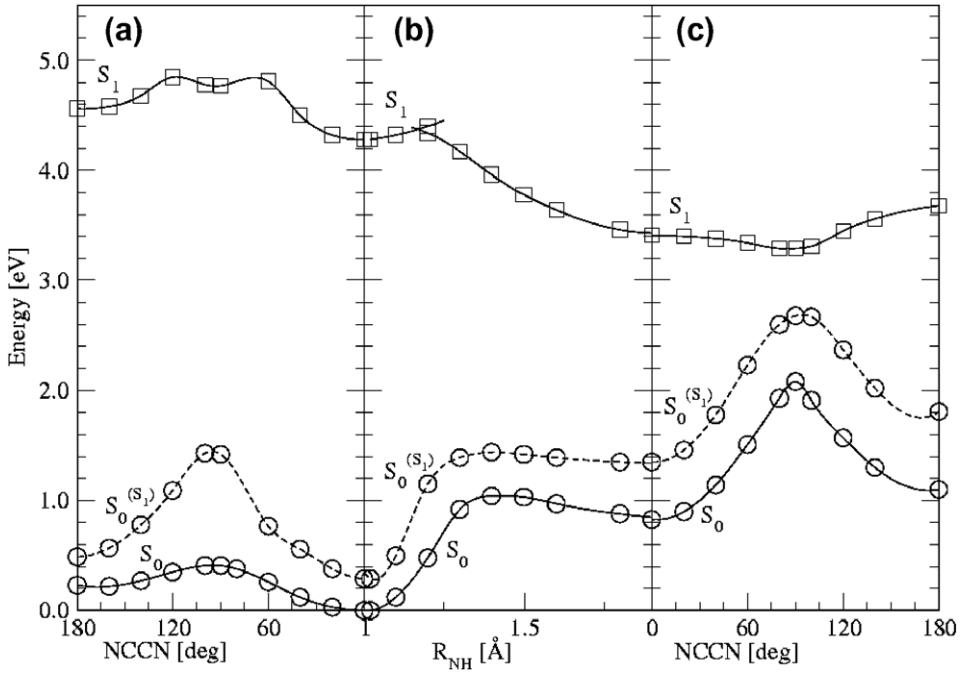

Fig. 6. Potential-energy energy profiles of the S_0 state (circles) and the $S_1(\pi\pi^*)$ state (squares) of 2-(2′-pyridyl)pyrrole as a function of the torsional reaction path (a, c) and the hydrogen-transfer reaction path (b). Full lines: energy profiles of reaction paths determined in the same electronic state. The dashed lines denote the energy of the ground state calculated at the geometry of the S_1 state (designated as $S_0^{(S_1)}$).

Geometry / Orbital	(a) S_0 min of N form	(b) $^1\pi\pi^*$(C_s min) of T form	(c) $^1\pi\pi^*$(C_1 min) of T form
π^*_{L+1}	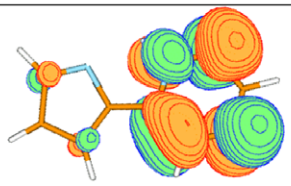	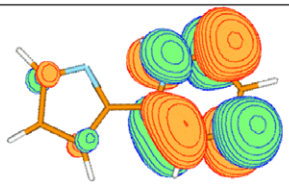	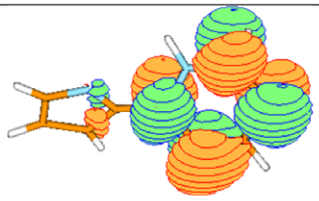
π^*_{L}	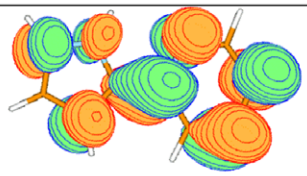	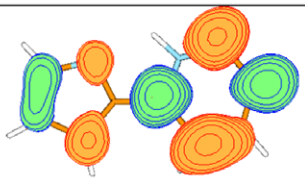	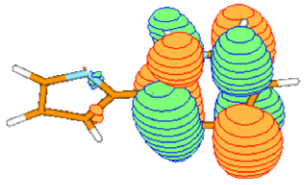
π_{H}	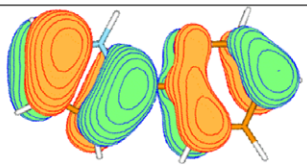	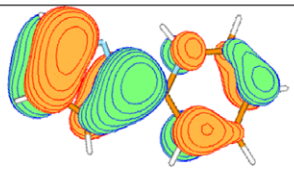	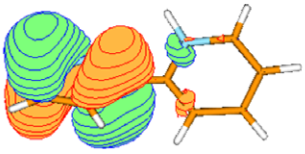
π_{H-1}	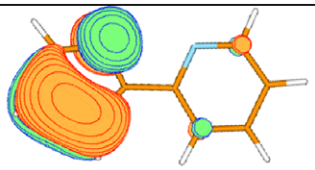	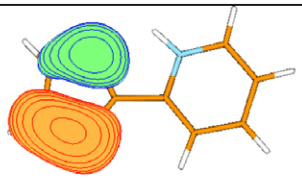	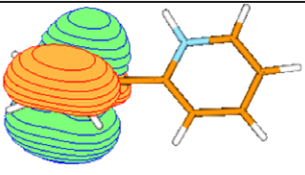

Fig. 7. The highest occupied (π_{H-1} and π_H) and the lowest unoccupied (π^*_L and π^*_{L+1}) orbitals of 2-(2′-pyridyl)pyrrole, determined at: the equilibrium geometry of the electronic ground state (a), the equilibrium geometry of the S_1 state (b), and near the S_1-S_0 intersection (c).

tion at the CASSCF level. The resulting geometry is shown in Fig. 5d. The characteristic features of this geometry are the twist angle of 86° and the piramidization of the N_{pyrid} atom (the sum of the bond angles is 349°). The hydrogen bond distance is elongated in this structure to 3.152 Å and the hydrogen atom sticks out of the pyridine ring plane by the angle of 143°.

To provide insight into the electronic structure of the states involved in the photophysics of 2PP, we display in Fig. 7 the frontier orbitals; HOMO (π_H), HOMO-1 (π_{H-1}), LUMO (π^*_L) and LUMO+1 (π^*_{L+1}), which are involved in the $S_0 \rightarrow S_1$ electronic excitation, at the planar S_0 equilibrium geometry (a), the hydrogen-transferred S_1 state (b) and at the perpendicular geometry ($\theta = 90°$) close to expected S_1–S_0 conical intersection (c). Upon inspection of results shown in Table 2 one can notice that only π_H, π^*_L and π^*_{L+1} orbitals of the aromatic rings are involved as frontier orbitals in the S_1 state. It can be seen that the $S_0 \rightarrow S_1$ excitation at the S_0 equilibrium geometry is accompanied by a small shift of electron density from the pyrrole ring to the pyridine ring (Fig. 7a). At the S_1 minimum, the ground state is highly polar ($\mu = 11.2$ D for the perpendicular arrangement of the rings and 6.2 D for the planar minimum) due to the nearly complete localization of the π_H orbital on the pyrrole ring (c.f. Fig. 7b and c), whereas the proton has been transferred to the pyridine ring. This polarity is strongly reduced in the S_1 state ($\mu = 3.1$ D for the perpendicular and 2.3 D for the planar S_1 minimum) due to the LUMOs which are mostly localized on the pyridine ring. At the geometry close to the S_1–S_0 conical intersection, the HOMOs and LUMOs are completely localized on pyrrole and pyridine, respectively (Fig. 7c). 2PP at this configuration thus is an almost perfect biradical, as is typical for a degeneracy of the open-shell S_1 state with the closed-shell ground state [18].

While in intermolecularly hydrogen-bonded aromatic systems the hydrogen-transfer process leads directly to a conical intersection with the electronic ground state (cf. Fig. 4), this is not the case in intramolecularly hydrogen-bonded π systems, see Fig. 6b. A very similar picture as in Fig. 6 has also been found for the ESIPT systems salicylic acid [31], 2-(2′-hydroxyphenyl)benzotriazole (HBT) [32], and for 7-(2′-pyridyl)indole [33]. It seems thus generic that intramolecularly hydrogen-bonded aromatic systems require a torsional motion to reach the conical intersection of the S_1 and S_0 surfaces, where the radiationless deactivation takes place.

4. Conclusions

We have discussed in this article generic mechanisms of excited-state deactivation via hydrogen-atom dynamics in a hydrogen-bonded pair of aromatic chromophores and in a bifunctional intramolecularly hydrogen-bonded aromatic system. It has been shown that an excited-state reaction involving the transfer of a hydrogen atom plays a decisive role for the photophysics of these systems. The overall radiationless deactivation process for the hydrogen-bonded system discussed above may be characterized as an electron-driven proton-transfer (EDPT) mechanism. The only qualitative difference between the systems where the PD and PA moieties are connected by an inter-molecular (PP) and an intra-molecular (2PP) hydrogen bond, respectively, is that in the latter system the PT reaction takes place on the adiabatic PE surface of the S_1 state, while a non-adiabatic LE-CT transition is necessary in the former case [33]. Once the CT state is populated, the proton moves from the donor atom towards the acceptor atom, following the electron; after the back-transfer of the electron at the conical intersection of the CT state with the S_0 state, the proton is driven back to the original location. This way, the energy of the UV photon is converted into vibrational energy of the hydrogen bond, which subsequently is dissipated to other intramolecular as well as intermolecular vibrational degrees of freedom. The unusually large electronic energy gradients and the small mass of the proton ensure the exceptionally fast (sub-picosecond) rate of this process.

In planar intramolecularly hydrogen-bonded π-systems, the excited-state hydrogen transfer itself does not lead to a S_1–S_0 conical intersection. However, there is now compelling evidence from the computational investigation of several characteristic ESIPT systems that the hydrogen-transfer process triggers an out-of-plane torsion on the S_1 surface which leads in a barrierless manner to a S_1–S_0 conical intersection and thus ultrafast internal conversion [31–33].

Our results suggest that the EDPT process is responsible for fluorescence quenching by hydrogen bonding, the function of commercial organic photostabilizers, and the photostability of biological molecules such as DNA and proteins [34].

Acknowledgements

This work has been supported by the research Grant of the Ministry of Science and Education of Poland (3 T09A 107 28) and the Grant of the Interdisciplinary Center of Mathematical and Computer Modeling (ICM) of Warsaw University (Grant No. G29-11).

Appendix A. Supplementary data

Supplementary data associated with this article can be found, in the online version, at doi:10.1016/j.chemphys.2007.11.013.

References

[1] G.C. Pimentel, A.L. McClellan, The Hydrogen Bond, Freeman, San Francisco, 1960.
[2] S.J. Formosinho, L.G. Arnaut, J. Photochem. Photobiol. A 75 (1993) 21.
[3] S.M. Ormson, R.G. Brown, Progr. React. Kin. 19 (1994) 45; D. Le Gourrierec, S.M. Ormson, G.G. Brown, Progr. React. Kin. 19 (1994) 211.

[4] A. Douhal, F. Lahmani, A.H. Zewail, Chem. Phys. 207 (1996) 477.
[5] H.J. Heller, H.R. Blattmann, Pure Appl. Chem. 30 (172) 145; H.J. Heller, H.R. Blattmann, Pure Appl. Chem. 36 (1974) 141.
[6] J.-E.A. Otterstedt, J. Chem. Phys. 58 (1973) 5716.
[7] D. Rehm, A. Weller, Isr. J. Chem. 8 (1970) 259.
[8] L.G. Arnaut, S.J. Formosinho, J. Photochem. Photobiol. A 75 (1993) 1.
[9] N. Mataga, Adv. Chem. Phys. 107 (1999) 431.
[10] J. Waluk, Acc. Chem. Res. 36 (2003) 832.
[11] O. Christiansen, H. Koch, P. Jørgensen, Chem. Phys. Lett. 243 (1995) 409.
[12] C. Hättig, F. Weigend, J. Chem. Phys. 113 (2000) 5154.
[13] A. Köhn, C. Hättig, J. Chem. Phys. 119 (2003) 5021.
[14] D.E. Woon, T.H. Dunning Jr., J. Chem. Phys. 98 (1993) 1358.
[15] R. Ahlrichs, M. Bär, M. Häser, H. Horn, C. Kölmel, Chem. Phys. Lett. 162 (1989) 165.
[16] F. Weigend, M. Häser, Theor. Chem. Acc. 97 (1997) 331.
[17] M.J. Frisch, G.W. Trucks, H.B. Schlegel, G.E. Scuseria, M.A. Robb, J.R. Cheeseman, J.A. Montgomery Jr., T. Vreven, K.N. Kudin, J.C. Burant, J.M. Millam, S.S. Iyengar, J. Tomasi, V. Barone, B. Mennucci, M. Cossi, G. Scalmani, N. Rega, G.A. Petersson, H. Nakatsuji, M. Hada, M. Ehara, K. Toyota, R. Fukuda, J. Hasegawa, M. Ishida, T. Nakajima, Y. Honda, O. Kitao, H. Nakai, M. Klene, X. Li, J.E. Knox, H.P. Hratchian, J.B. Cross, V. Bakken, C. Adamo, J. Jaramillo, R. Gomperts, R.E. Stratmann, O. Yazyev, A.J. Austin, R. Cammi, C. Pomelli, J.W. Ochterski, P.Y. Ayala, K. Morokuma, G.A. Voth, P. Salvador, J.J. Dannenberg, V.G. Zakrzewski, S. Dapprich, A.D. Daniels, M.C. Strain, O. Farkas, D.K. Malick, A.D. Rabuck, K. Raghavachari, J.B. Foresman, J.V. Ortiz, Q. Cui, A.G. Baboul, S. Clifford, J. Cioslowski, B.B. Stefanov, G. Liu, A. Liashenko, P. Piskorz, I. Komaromi, R.L. Martin, D.J. Fox, T. Keith, M.A. Al-Laham, C.Y. Peng, A. Nanayakkara, M. Challacombe, P.M.W. Gill, B. Johnson, W. Chen, M.W. Wong, C. Gonzalez, J.A. Pople, Gaussian, Inc., Wallingford CT, 2004.
[18] M. Klessinger, J. Michl, Excited States and Photochemistry of Organic Molecules, VCH, Weinheim, 1995.
[19] N. Mataga, S. Tsuno, Bull. Chem. Soc. Jpn. 30 (1957) 711.
[20] J. Herbich, M. Kijak, A. Zielinska, R.P. Thummel, J. Waluk, J. Phys. Chem. A 106 (2002) 2158.
[21] M. Kijak, Y. Nosenko, A. Singh, R.P. Thummel, J. Waluk, J. Am. Chem. Soc. 129 (2007) 2738.
[22] A.L. Sobolewski, W. Domcke, Chem. Phys. 294 (2003) 73.
[23] A.L. Sobolewski, W. Domcke, C. Hättig, Proc. Nat. Acad. Sci. 102 (2005) 17903.
[24] S. Perun, A.L. Sobolewski, W. Domcke, J. Phys. Chem. 110 (2006) 9031.
[25] T. Schultz, E. Somoylova, W. Radloff, I.V. Hertel, A.L. Sobolewski, W. Domcke, Science 306 (2004) 1765.
[26] A. Abo-Riziq, L. Grace, E. Nir, M. Kabelac, P. Hobza, M.S. de Vries, Proc. Natl. Acad. Sci. USA 102 (2005) 20.
[27] N.K. Schwalb, F. Temps, J. Am. Chem. Soc. 129 (2007) 9272.
[28] Y. Nosenko, Y. Stepanenko, F. Wu, R.P. Thummel, A. Mordzinski, Chem. Phys. Lett. 315 (1999) 87.
[29] A. Kyrychenko, J. Herbich, F. Wu, R.P. Thummel, J. Waluk, J. Am. Chem. Soc. 122 (2000) 2818.
[30] G. Wiosna, I. Petkova, M.S. Mudadu, R.P. Thummel, J. Waluk, Chem. Phys. Lett. 400 (2004) 379.
[31] A.L. Sobolewski, W. Domcke, Phys. Chem. Chem. Phys. 8 (2006) 3410.
[32] A.L. Sobolewski, W. Domcke, C. Hättig, J. Phys. Chem. A 110 (2006) 6301.
[33] A.L. Sobolewski, W. Domcke, J. Phys. Chem. 111 (2007) 11725.
[34] A.L. Sobolewski, W. Domcke, Europhysicsnews 37 (2006) 20.